ISTITUTO NAZIONALE DI FISICA NUCLEARE
Laboratori Nazionali di Frascati

LNF-84/30

S.R.Amendolia et al.: MEASUREMENT OF THE PION FORM FACTOR IN THE TIME-LIKE REGION FOR q^2 VALUES BETWEEN 0.1 $(GeV/c)^2$ AND 0.18 $(GeV/c)^2$

Estratto da:
Phys. Letters 138B, 454 (1984)

Servizio Documentazione
dei Laboratori Nazionali di Frascati

MEASUREMENT OF THE PION FORM FACTOR IN THE TIME-LIKE REGION FOR q^2 VALUES BETWEEN 0.1 (GeV/c)^2 AND 0.18 (GeV/c)^2

S.R. AMENDOLIA [c], B. BADELEK [c], G. BATIGNANI [f], G.A. BECK [e], E.H. BELLAMY [g], E. BERTOLUCCI [c], D. BETTONI [c], H. BILOKON [e], A. BIZZETI [c], G. BOLOGNA [e], L. BOSISIO [c], C. BRADASCHIA [c], M. BUDINICH [f], M. DELL'ORSO [c], B. D'ETTORRE PIAZZOLI [e], M. ENORINI [a], F.L. FABBRI [a], F. FIDECARO [g], L. FOÀ [c], E. FOCARDI [c], S.G.F. FRANK [d], P. GIANNETTI [c], A. GIAZOTTO [c], M.A. GIORGI [c], J. HARVEY [d], G.P. HEATH [g], M.P.J. LANDON [g], P. LAURELLI [a], F. LIELLO [f], G. MANNOCCHI [e], P.V. MARCH [g], P.S. MARROCCHESI [c], D. MENASCE [b], A. MENZIONE [c], E. MERONI [b], E. MILOTTI [f], L. MORONI [b], P. PICCHI [e], F. RAGUSA [f], L. RISTORI [c], L. ROLANDI [f], C. SALTMARSH [g], A. SAOUCHA [g], L. SATTA [a], A. SCRIBANO [c], A. STEFANINI [f], J.A. STRONG [g], R. TENCHINI [c], G. TONELLI [c], G. TRIGGIANI [c] and A. ZALLO [a]

[a] *INFN-Laboratori di Frascati, Frascati, Italy*
[b] *Dipartimento di Fisica and Sezione INFN, Milan, Italy*
[c] *Dipartimento di Fisica, Sezione INFN and Scuola Normale Superiore, Pisa, Italy*
[d] *Department of Physics, University of Southampton, England*
[e] *Istituto di Fisica Generale and Istituto di Cosmogeofisica del CNR, Turin, Italy*
[f] *Istituto di Fisica, Sezione INFN and Scuola Internazionale Superiore di Studi Avanzati, Trieste, Italy*
[g] *Department of Physics, Westfield College, London, England*

Received 9 January 1984

The EM form factor of the pion has been studied in the time-like region by measuring $\sigma(e^+e^- \to \pi^+\pi^-)$ normalized to $\sigma(e^+e^- \to \mu^+\mu^-)$. Results have been obtained for q^2 down to the physical threshold.

We report here results of an experiment performed at the CERN SPS by the NA7 collaboration to measure the pion form factor in the time-like region for q^2 values from threshold up to 0.18 (GeV/c)^2.

Existing information on the pion form factor in the time-like region below a q^2 of 0.5 (GeV/c)^2 is poor, and in the range covered by the present experiment only one point has been measured at a q^2 of 0.16 (GeV/c)^2, and with a 20% error [1]. Other data at lower q^2 come from indirect measurements and are model dependent [2]. The importance of a measurement of the pion form factor in the low q^2 region has been stressed several times, not only to measure the coupling of the time-like photon to the hadronic current in this region, but also to improve the hadronic correction to the calculation of $(g-2)$ for the muon [3].

Experimentally, the form factor is most easily determined by measuring simultaneously the cross sections for the reactions $e^+e^- \to \pi^+\pi^-$ and $e^+e^- \to \mu^+\mu^-$ since

$$|F(q^2)|^2 = C(q^2)\,\sigma(e^+e^- \to \pi^+\pi^-)/\sigma(e^+e^- \to \mu^+\mu^-),$$

where C is a factor dependent only on the π and μ masses and on q^2, but which includes radiative corrections. However, the predominant terms in the radiative corrections cancel out in this ratio and only minor contributions, of the order of a few percent, remain.

Fig. 1 shows the experimental apparatus. A positron beam was incident on a 28 cm long liquid hydrogen target. Data were taken at 100, 125, 150 and 175 GeV/c beam momentum. A differential Čerenkov

0.370-2693/84/$ 03.00

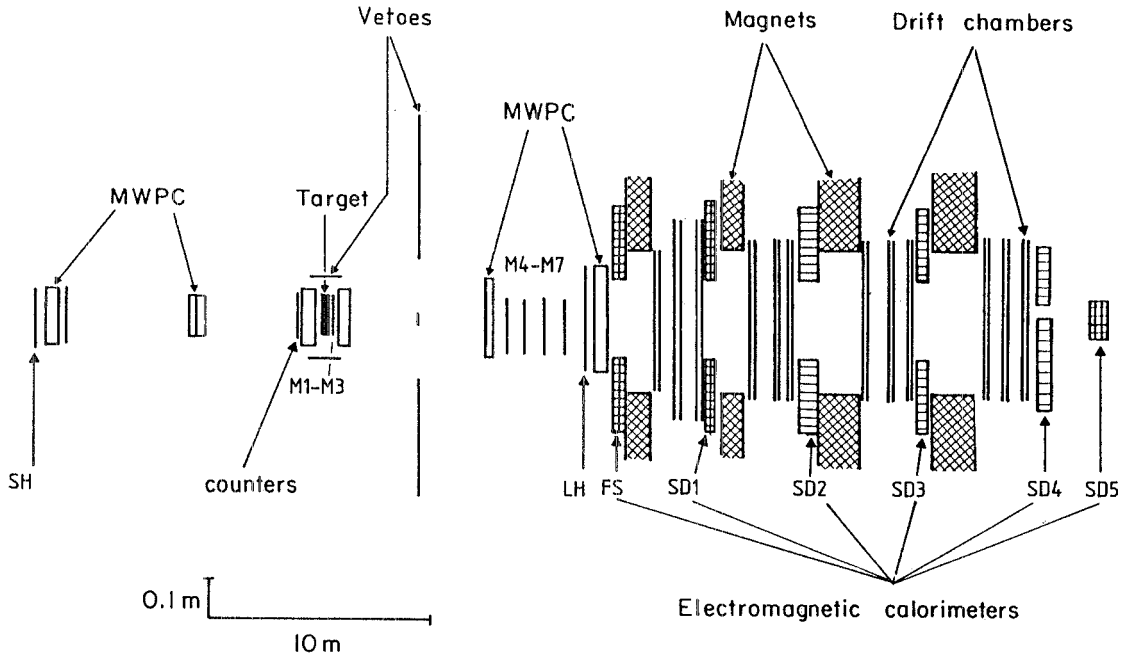

Fig. 1. The experimental apparatus.

counter (CEDAR), not shown in the figure, was used to flag the incoming particle and thus to discriminate between positrons and the hadronic component (30%) of the beam. Scintillation counters vetoed the beam halo and the hodoscope SH rejected events with more than one incoming particle. Veto counters rejected events with particles at angles larger than 5 mrad. The hodoscope LH together with counters M1–M7 performed a charge multiplicity analysis of the final state for triggering purposes.

Two sets of MWPC (8 planes of 1 mm spaced wires within a 25 cm^2 sensitive region) upstream of the target measured the direction of the incoming particle with an accuracy of 0.02 mrad. Downstream of the target, three more sets of similar MWPC (400 cm^2 sensitive region) measured the directions of outgoing particles with the same accuracy. Downstream of the LH hodoscope the FRAMM magnetic spectrometer measured the momenta of final state particles. It consisted of 4 magnets interspaced with sets of drift chambers and shower detectors (SD). The latter formed part of the trigger and were also used to identify and thus reject events containing electrons. A detailed description of the spectrometer can be found elsewhere [4]. In this geometry its angular acceptance is limited to ±7 mrad.

The multiwire chambers defined the vertex from the incoming positron and two outgoing particles. The vertex position was used to reject events with an interaction point falling outside the target. An event was also rejected if the sum of θ_1 and θ_2, the scattering angles of the two particles, was less than 0.4 mrad.

In fig. 2a experimental data at 150 GeV/c are presented in a plot of θ_1 versus θ_2. For the sake of clarity fig. 2 presents only a part of the available statistics. Events cluster around the kinematic curves for the processes $e^+e^- \to \pi^+\pi^-$, $e^+e^- \to \mu^+\mu^-$, and $e^+e^- \to e^+e^-$ (Bhabha scattering).

Most of the background is concentrated along the axes, typically beam plus one scattered δ-ray or beam plus one slow particle arising from the conversion of a low energy photon radiated by the positron. This background was removed by measuring the multiplicity of tracks reconstructed by the spectrometer since the low momentum particle was swept away from the downstream detectors by the first magnet. Fig. 2b shows the θ_1 versus θ_2 plot for events which have one fitted track in these detectors, and fig. 2c

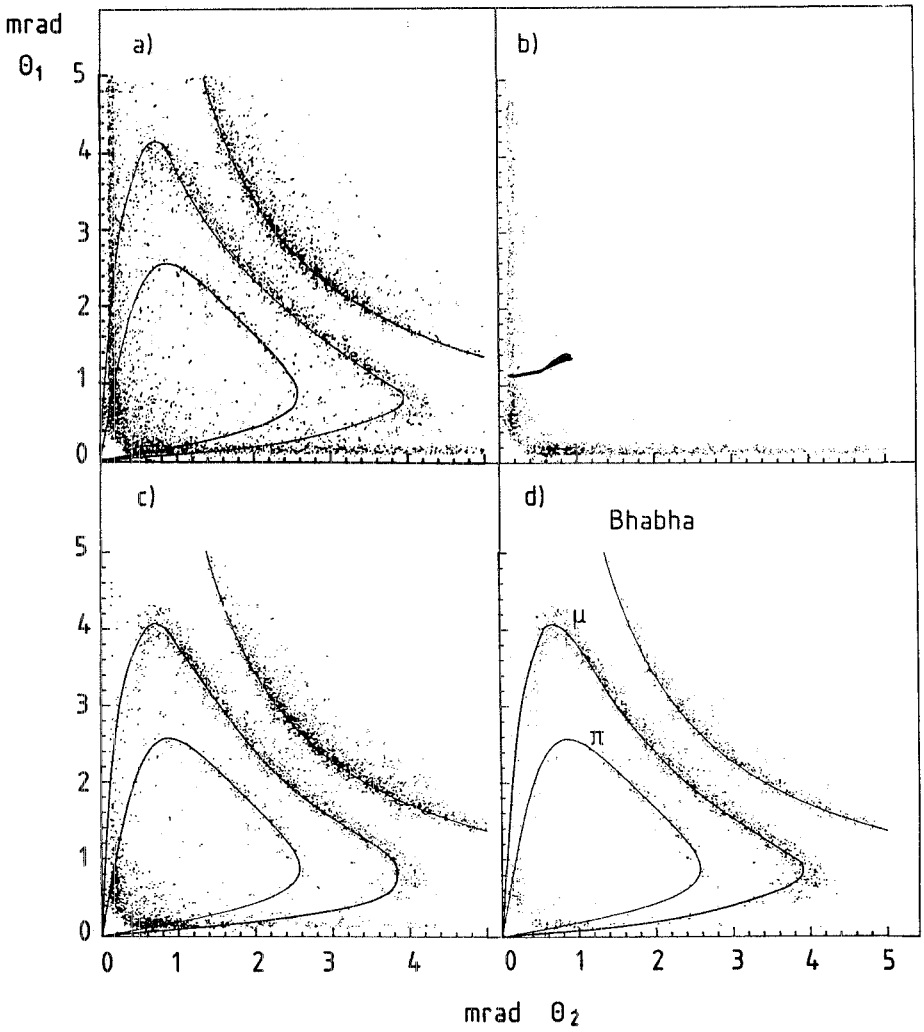

Fig. 2. θ_1 versus θ_2 at 150 GeV/c. (a) Raw data. (b) Events with multiplicity 1. (c) Events with multiplicity 2 and total charge 0 in the magnetic spectrometer. (d) Data after the SD cut.

events with two tracks of opposite charge for the same sample of data. Imposing these cuts in multiplicity results in a loss of 5% of μ and π events.

The remaining background, especially at low q^2, was further reduced by means of the information from the shower detectors, which were split longitudinally into two parts of 4 and 20 radiation lengths. A charged particle was identified as an electron if there was a large energy release in the front part and if the shower energy corresponded to the magnetically measured momentum. Events were rejected if both particles were identified as electrons. The retention of events with only one particle showing an electron signature limits the loss of pion pairs to less than 1.5%. This is the only selection criterion which can cause the loss of pions while leaving the muon sample unaffected. This procedure also accounts for the residual Bhabha signal which is still present in the final data sample.

Fig. 2d shows the resulting θ_1 versus θ_2 plot. The separation between muons and pions is clear over most of the plot, and misidentification occurs only in the region near the axes (i.e. for values of scattering angle in the CM system around 0 and around π)

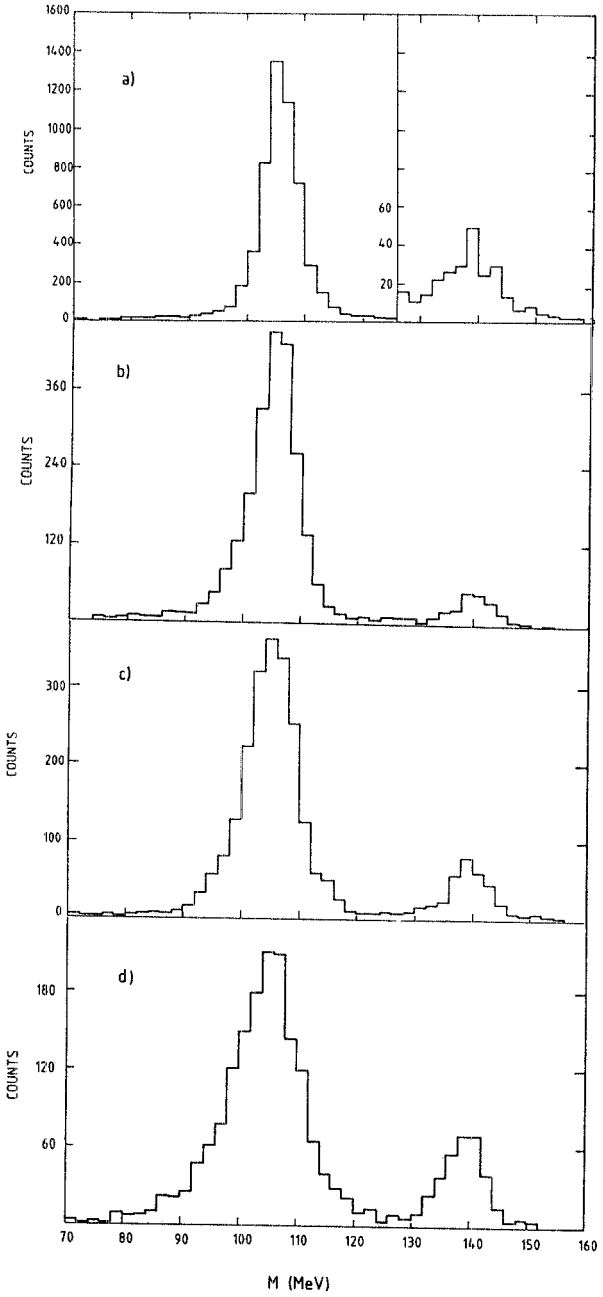

Fig. 3. Mass variable distributions. (a) 100 GeV/c. (b) 125 GeV/c. (c) 150 GeV/c. (d) 175 GeV/c.

where the curves for the two interactions are not well resolved. We therefore use only the region of the plot corresponding to both particles having scattering angles greater than 0.7 mrad. Since the angular distributions in the CM system for both reactions are known, the correction for events with one angle less than 0.7 mrad (always less than 20%) can be readily applied.

There is also a very low diffuse background still present in the central region of the plot. The θ_1 versus θ_2 plot can be converted to a mass plot using the relation

$$M = \tfrac{1}{2}\,[2mP(1-(\theta^+/\theta^-)^2)(1-\theta_1\theta_2 P/2m)]^{1/2},$$

where M is the mass of the particle in the reaction $e^+e^- \to M^+M^-$, P is the momentum of the incident particle, m the electron mass, and $\theta^+ = \theta_1 + \theta_2$ and $\theta^- = \theta_1 - \theta_2$. Fig. 3 shows the data collected at each energy in terms of this variable. As expected, clustering along kinematic curves in the θ_1 versus θ_2 plot results in peaks at the corresponding masses of the produced particle. The plot allows the determination of the background levels at each energy. The resulting numbers of pion and muon pairs are given in table 1.

To compute the pion form factor, corrections to the data to account for the following effects have been applied:

(a) Energy independent factors:

(i) Interaction of pions in the material of the spectrometer (12.3% at all energies).

(ii) Misidentification of pion pairs as electron pairs in the shower detectors (1.5%).

(iii) Inefficiency in matching the charged tracks reconstructed in the spectrometer with the energy released in the shower detectors (2.5%).

(b) Energy dependent factors:

(i) Energy dispersion of the positron beam due to radiation of photons upstream of the target.

(ii) The ratio of radiative corrections for pion and muon pairs.

The increase in these corrections towards the

Table 1
Number of pion and muon pairs.

Beam momentum (GeV/c)	$N(\pi)$	$N(\mu)$	Statistical error (%)	Systematic error (%)
100	217	5681	6.7	5.0
125	209	2309	7.0	2.5
150	324	2050	6.0	2.0
175	350	1525	6.0	1.0

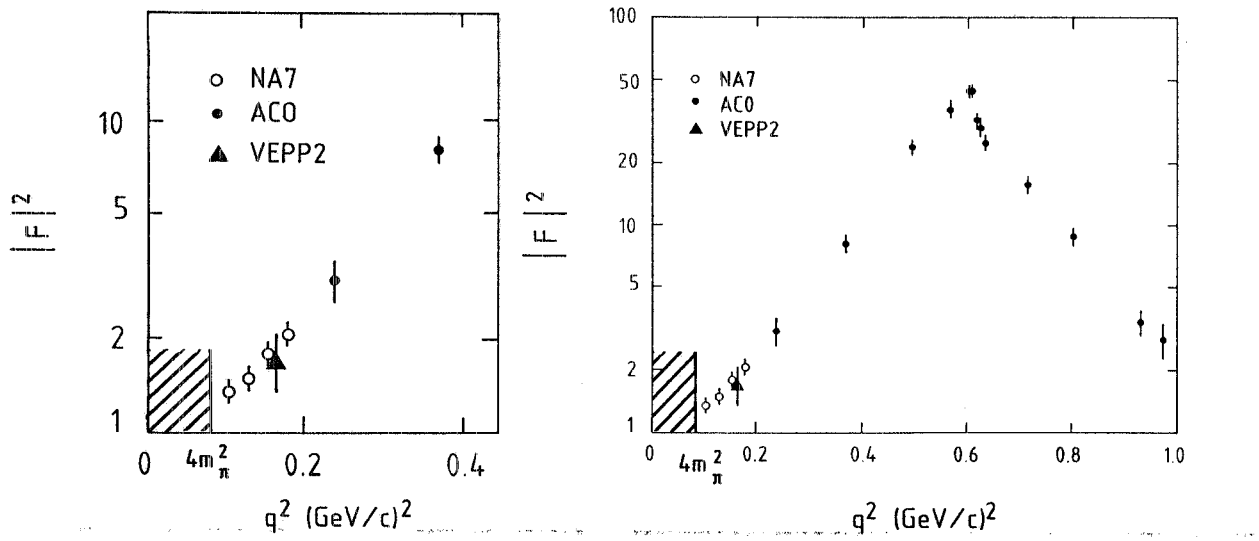

Fig. 4. The pion form factor squared.

Table 2
Correction factors to $N(\pi)/N(\mu)$.

Beam momentum (GeV/c)	Radiative corrections	Energy dispersion of the beam
100	1.0160	1.040
125	1.0064	1.012
150	1.0035	1.007
175	1.0023	1.005

Table 3
The pion form factor squared.

Beam momentum (GeV/c)	q((GeV/c)^2)	$[F(q^2)]^2$
100	0.101	1.35 ± 0.09
125	0.127	1.48 ± 0.1
150	0.152	1.78 ± 0.1
175	0.178	2.05 ± 0.12

$\pi^+\pi^-$ threshold (particularly at 100 GeV), is due to the increasing difference between the production cross section for π and μ pairs and the fast rise in π pair production at threshold.

Table 2 summarizes the energy dependent correction factors.

The values obtained for the pion form factor are listed in table 3 and plotted in fig. 4. Statistical errors only are shown. No deviation from a smooth trend towards $F(0) = 1$ is suggested by our data which are in good agreement with those of previous experiments [1,5]. Forthcoming results of the NA7 measurement of the pion form factor in the space-like region will allow its precise determination close to $q^2 = 0$ and combined with the present results will permit a reliable interpolation through the unphysical region.

References

[1] I.B. Vasserman et al., Yad. Fiz. 30 (1979) 999.
[2] S.F. Berezhnev et al., Yad. Fiz. 26 (1977) 547.
[3] J. Calmet et al., Rev. Mod. Phys. 49 (1977) 21.
[4] E. Albini et al., Phys. Lett. 110B (1982) 339.
[5] A. Quenzer et al., Phys. Lett. 76B (1978) 512.